Acta Crystallographica Section D
Biological Crystallography
ISSN 0907-4449

A crystallographic glimpse of a nucleotide triphosphate (AMPPNP) bound to a protein surface: external and internal AMPPNP molecules in crystalline *N*-acetyl-L-glutamate kinase

Fernando Gil-Ortiz,[a] Ignacio Fita,[b] Santiago Ramón-Maiques,[a] Alberto Marina[a]† and Vicente Rubio[a]*

[a]Instituto de Biomedicina de Valencia, Consejo Superior de Investigaciones Científicas (IBV-CSIC), C/Jaime Roig 11, 46010-Valencia, Spain, and [b]Instituto de Biología Molecular de Barcelona (IBMB-CSIC), C/Jordi Girona 18-21, 08034-Barcelona, Spain

† Present address: Department of Biochemistry and Molecular Biophysics, Columbia University, New York, NY 10032, USA.

Correspondence e-mail: rubio@ibv.csic.es

Received 15 April 2002
Accepted 30 July 2002

A large volume of unexplained electron density in the crystal of *N*-acetyl-L-glutamate kinase (NAGK) is now interpreted as an external, very extended, metal-free AMPPNP molecule that occupies two alternative positions and that makes contacts with the protein exclusively through its γ-imidophosphate. This external nucleotide is compared with the active-site nucleotide and the reasons for its extended shape, lack of complexed metal and peripheral binding are analyzed. Further, the possibility that this bystander AMPPNP is waiting to occupy the active centre is discussed.

1. Introduction

The crystal structure (Ramón-Maiques *et al.*, 2002) to 1.5 Å of the complex with *N*-acetyl-L-glutamate (NAG) and MgAMPPNP of *Escherichia coli N*-acetyl-L-glutamate kinase (NAGK), the enzyme that catalyzes the second and frequently controlling step of the route of arginine biosynthesis (Cunin *et al.*, 1986), revealed that NAGK is a homodimer nucleated by a molecular 16-stranded open β-sheet sandwiched between α-helices. In each subunit, an N-terminal lobe binds NAG and forms the dimer interface and the C-lobe binds the ADP moiety of MgAMPPNP. The nucleotide lies extended along the sheet C-edge, with the γ-phosphoryl appropriately oriented for transfer to the NAG γ-carboxylate.

An unresolved aspect of the NAGK crystal structure was a large volume of electron density localized over the dyadic axis of the NAGK homodimer that could not be interpreted on the basis of the NAGK polypeptide-chain model. This electron density is shown here to arise from an external AMPPNP molecule that occupies two alternative positions around a crystal symmetry twofold axis coincident with the molecular dyad axis. The position of this nucleotide made it conceivable that it was waiting to occupy the nucleotide site at the active centre, but the chemical characteristics of this nucleotide differ from those of the active-centre-bound nucleotide, rendering this possibility unlikely. The reasons for the conformational stability of this nucleotide and its fixed localization in the protein crystal, as well as for its lack of Mg^{2+} complexation despite the abundance of $MgCl_2$ in the crystal mother liquor, are also discussed.

2. Experimental methods

NAGK expression, purification and crystallization at pH 4.6 as the ternary complex with AMPPNP and NAG and its structure determination at 100 K to 1.5 Å resolution at beamline ID14-1 at ESRF, Grenoble have previously been described (Gil *et al.*, 1999; Ramón-Maiques *et al.*, 2002). The crystals (space group $C222_1$; unit-cell parameters a = 59.4, b = 71.7, c = 107.3 Å) contain one protein subunit in the asymmetric unit with about 50% solvent. The final model (PDB code 1gs5) of the ternary NAGK–AMPPNP–NAG complex (with agreement values of R = 20.88% and $R_{\rm free}$ = 21.28% and good stereochemistry) corresponds to a monomer including all protein residues (Met1–Pro258), 198 water molecules and one bound molecule each of NAG and MgAMPPNP. In addition, a large volume of electron density located in the vicinity of the crystallographic twofold axis coincident with the molecular dyad axis (Fig. 1*a*) is now interpreted as an AMPPNP molecule. A few cycles of model building with *O* (Jones *et al.*, 1991) and of refinement with *REFMAC* (Murshudov *et al.*, 1997) were carried out to construct the model for this extra AMPPNP. Bond lengths and angles for this modelled nucleotide fall in all cases within the expected ranges for AMPPNP (Saenger, 1984). Difference and omit Fourier electron-density maps (Fig. 1*b*) were computed to cross-check the reliability of the proposed interpretation, particularly taking into account possible phasing artifacts arising from the proximity of the crystallographic symmetry axis. Figures were drawn with *MOLSCRIPT* (Kraulis, 1991), *BOBSCRIPT* (Esnouf, 1999), *Raster3D*

(Merritt & Murphy, 1994) and *DINO* (Phillippsen, 1998).

3. Results

3.1. An AMPPNP molecule best explains the external density

A large volume (~150 Å^3) of electron density, having in projection a frog-like appearance (Fig. 1*a*), located between different enzyme molecules at the crystallographic twofold axis corresponding to the dimer dyadic axis, contacts NAGK through the lower part of the density (the frog legs) at the connection of helix αB with strand β3 (Fig. 1*a*). No such density has been observed in isomorphous crystals of the enzyme grown in the presence of ADP (data not shown). An external AMPPNP molecule having two symmetric conformations, each with 50% occupancy, accounts for this electron density (Ghosh *et al.*, 2000), which is of comparable density to the protein, and for the continuity of the density across the twofold symmetry axis (Fig. 1*b*). The adenine and the ribose, overlapping with the symmetrically related alternative position, fit the frog head and body and the two alternative positions of the AMPPNP fit within the rear frog legs. Some of the atoms are situated near the surface of the density map (Fig. 1*b*; in blue) These correspond to electronically light atoms that do not overlap with the symmetry-related molecule. The difference Fourier $F_o - F_c$ map computed in the presence of this AMPPNP confirms the quality of the fit (Fig. 1*b*; in red). The only positive densities in the difference map are the two symmetrical peaks that evoke the frog front legs, possibly corresponding to either solvent molecules or to an alternative conformation of the adenosine moiety having low occupancy. *R* values remain essentially unchanged with the introduction of the model.

3.2. Conformation of the external AMPPNP compared with that of active-site AMPPNP

The external AMPPNP molecule (Figs. 1*b* and 1*c*) presents good stereochemistry (Saenger, 1984) and has a conformation expected to be highly stable in solution. The adenine ring is *anti* (χ = 140°), the ribose exhibits a C3′-*endo* pucker (pseudorotation angle value P = 23°) and the γ torsion angle (C4′—C5′ bond) is in the limit for −synclinal (−97°), allowing the staggering of C4′ and C5′ substituents and appropriately orienting the 3′ and 5′ O ribose atoms for formation of an internal canonical hydrogen bond (Fig. 1*c*) that may contribute importantly to the stability of the nucleotide extended form. Torsion angle β (C5′—O5′bond) is antiperiplanar (154°) and the α and β phosphates are staggered, while the β and γ phosphates approach the stable eclipsed conformation with no short contacts, possibly resulting from interactions with the protein. No electron density attributable to a complexed Mg^{2+} was observed in maps

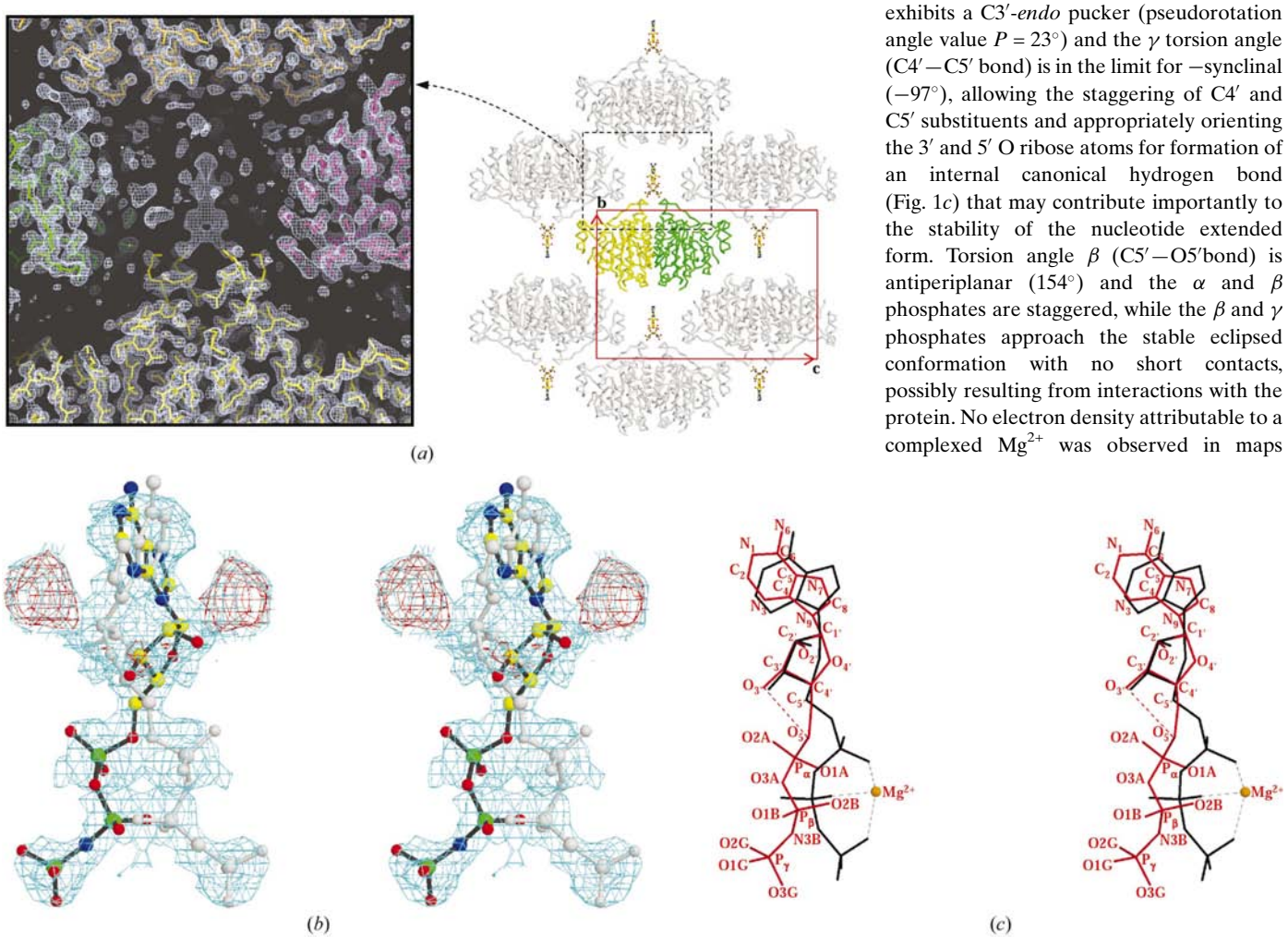

Figure 1
(*a*) Left panel: $2F_o - F_c$ map showing the unexplained electron density, having in projection a frog-like appearance, among four different enzyme molecules (bonds modelled in different colours) corresponding to the region enclosed in the broken-line rectangle of the right panel. This panel represents the crystal packing of the protein (in backbone representation) and also, in colour, the external AMPPNP modelled in the previously unexplained density. One enzyme dimer is also coloured within the unit cell, represented as a red rectangle. The *a* axis is perpendicular to the paper and thus is not shown. (*b*) Stereoview of $F_o - F_c$ frog-like electron density, obtained in the absence (in blue) or in the presence (in red) of the AMPPNP model. The AMPPNP model is shown in ball-and-stick representation, coloured in one of the two alternative conformations and grey in the other conformation. (*c*) Stereo comparison of the internal (in black) and external (in orange) AMPPNP, in bond representation. Atom nomenclature is also indicated. The intramolecular hydrogen bond is shown as a broken line in the external nucleotide. In the internal nucleotide, a Mg^{2+} ion is bound to the polyphosphate moiety in a tridentate coordination (broken black lines).

computed either without or with the nucleotide (Fig. 1*b*). At the 1.5 Å resolution of the present data, if Mg^{2+} were complexed it would have been observed, as it was the case for the internally bound nucleotide (Ramón-Maiques *et al.*, 2002). At pH 4.6 and the concentrations of 3 m*M* AMPPNP and 15 m*M* $MgCl_2$ used in the crystallization drop, ∼2/3 of the AMPPNP should not be complexed to Mg^{2+} {the apparent stability constant for the MgAMPPNP complex at pH 4.6 is $K'_{pH4.6} = 35\ M^{-1}$; calculated from $K'_{pH4.6} = K'_{pH8.5}/\delta$ (O'Sullivan & Smithers, 1979), where $\delta = [1 + 10^{(pK_a - 4.6)}]/[1 + 10^{(pK_a - 8.5)}]$, assuming a p$K_a$ of 7.7 for the γ-phosphate and a $K'_{pH8.5} = 38\,200\ M^{-1}$ for AMPPNP (Yount *et al.*, 1971)}.

The AMPPNP molecule bound at the active site is also highly extended (Ramón-Maiques *et al.*, 2002), but it differs importantly from the external AMPPNP molecule (Fig. 1*c*; Table 1). The adenine is in the *syn* configuration ($\chi = 63°$), the ribose exhibits a C4′-*exo* pucker (pseudorotation angle $P = 66°$) and the torsion angle γ is −antiperiplanar (−159°), allowing staggering of the C4′—C5′ substituents but preventing internal hydrogen-bond formation between the 3′ and 5′ O atoms. An Mg^{2+} ion is complexed with a non-bridging O atom from the three phosphates in Λ, *exo* conformation (Saenger, 1984), accounting for the eclipsed short contact conformation of Pα and Pβ and for the stable eclipsed conformation with no short contacts around the N atom bridging Pβ and Pγ.

Table 1
Conformation of the two independent AMPPNP molecules bound to NAGK.

Torsion angle‡	Defining atoms§	Torsion-angle value† (°) External AMPPNP	Active-site AMPPNP
	O3G, P_γ, N3B, P_β	−154	−180
	P_γ, N3B, P_β, O3A	−94	−123
	N3B, P_β, O3A, P_α	−94	103
	P_β, O3A, P_α, O_5	−81	103
α	O3A, P_α, $O_{5'}$, $C_{5'}$	−156	59
β	P_α, $O_{5'}$, $C_{5'}$, $C_{4'}$	154	75
γ	$O_{5'}$, $C_{5'}$, $C_{4'}$, $C_{3'}$	−97	−159
δ	$C_{5'}$,$C_{4'}$, $C_{3'}$, $O_{3'}$	75	86
χ	$O_{4'}$, $C_{1'}$, N_9, C_4	140 (*anti*)	63 (*syn*)
υ_0	$C_{4'}$, $O_{4'}$, $C_{1'}$, $C_{2'}$	0	−32
υ_1	$O_{4'}$, $C_{1'}$, $C_{2'}$, $C_{3'}$	−27	3
υ_2	$C_{1'}$, $C_{2'}$, $C_{3'}$, $C_{4'}$	41	24
υ_3	$C_{2'}$, $C_{3'}$, $C_{4'}$, $O_{4'}$	−42	−41
υ_4	$C_{3'}$, $C_{4'}$, $O_{4'}$, $C_{1'}$	28	48
P¶	Ribose conformation	23 (C3′-*endo*)	66 (C4′-*exo*)‡

† The *cis* conformation for successive bonds is given a zero value and positive and negative values are right and left-handed rotations, respectively. ‡ Nomenclature according to Arnott & Huckins (1969). § Atom nomenclature as defined in Fig. 1(*c*). ¶ Pseudorotation angle (P) is calculated (Altona & Sundaralingam, 1972) from the endocyclic sugar torsion angles as $\tan P = [(\upsilon_4 + \upsilon_1) - (\upsilon_3 + \upsilon_0)]/[2 \times \upsilon_2 \times (\sin 36° + \sin 72°)]$.

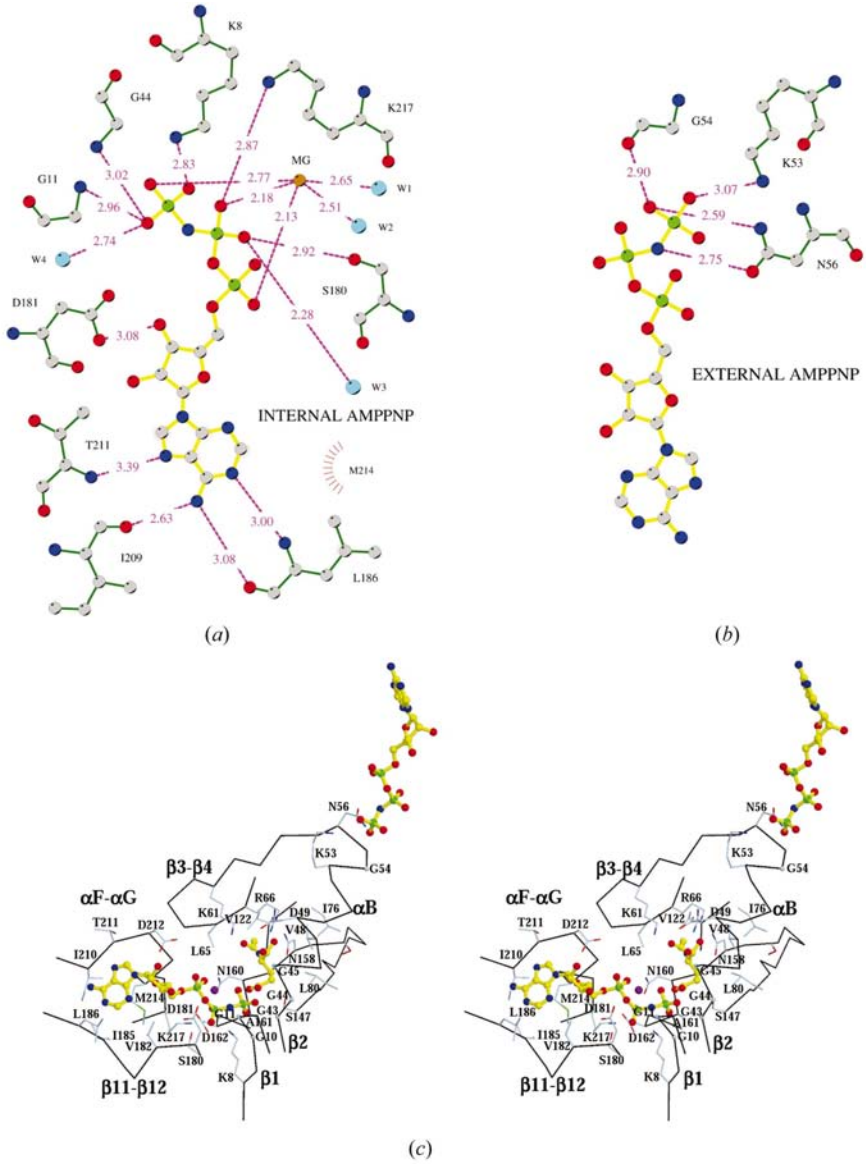

Figure 2
(*a*) and (*b*) Schematic plots drawn with *LIGPLOT* (Wallace *et al.*, 1995) of the interactions between the protein and the internal or external AMPPNP. Single-letter amino-acid codes are used for the protein residues. W denotes water molecules. MG denotes Mg^{2+}. Distances are in Å. (*c*) Stereoview of the C^α trace of the binding sites. AMPPNP and NAG are shown in ball-and-stick representation and coloured. Amino-acid side chains are in colour in a thinner trace.

3.3. Protein contacts of the external AMPPNP molecule

The interactions between the external nucleotide and the protein are mediated by the γ-imidophosphate (Fig. 2*b*): the bridging N atom (a hydrogen donor in this case) and the γ-phosphoryl O3G atom form hydrogen bonds with the Asn56 γ-amidic O and N atoms, respectively; the O3G atom, which is predominantly protonated at pH 4.6 (pK_a = 7.7; Yount *et al.*, 1971) is the donor in a hydrogen bond with the O atom of Gly54; the deprotonated O2G is a hydrogen acceptor and the countercharge for the N^ε atom of Lys53. The neutralization by the latter interaction of the negative charge on O2G should be critical to prevent repulsion with the negative C-end of the dipole at helix *B*.

4. Discussion

The extended configuration, orientation and localization of the external nucleotide relative to the active centre and the possibility of defining a direct path of approach without visible hindrances along the groove between helix αB and strand $\beta 3$ (Fig. 2*c*) might

suggest that the external nucleotide is waiting to occupy the active centre. However, the active centre and the peripheral site exhibit strong differential selectivity for the Mg-complexed and Mg-free forms of the nucleotide and there are important differences in conformation between the nucleotides bound at the two sites. Further, two of the four interactions between the peripheral nucleotide and the protein would not take place with ATP at neutral pH, since the hydrogen bonds involving the $\beta\gamma$ bridging N atom and the protonated O3G atom cannot be formed in the latter case and thus ATP may simply not bind peripherally at neutral pH. These facts cast strong doubts about the possibility of the external nucleotide being a precursor of the active-site nucleotide. In any case, the mainly free crystalline external AMPPNP offers a rare glimpse of this nucleotide in the solution as it approaches the enzyme.

5. Conclusions

In the crystal structure of NAGK at 1.5 Å resolution, a large volume of electron density has been interpreted as an extended AMPPNP molecule presenting two alternative dispositions around the twofold axis, with about half occupancy each. Unlike most protein-bound ATP molecules (Vetter & Wittinghofer, 1999), this AMPPNP is not metal-complexed and is mostly external to the protein, interacting with the latter only through its γ-imidophosphate. This external AMPPNP, although not appearing to be involved in the enzyme reaction, provides a glimpse of how free nucleotides can approach protein surfaces.

We thank the ESRF, Grenoble for the time at beamline ID14-1. We thank R. G. Yount for advice concerning the properties of AMPPNP. This work was supported by grants Rayos X of Fundación Ramón Areces and GV01-259 from the Generalitat Valenciana. FG-O and SR-M are fellows of the Fundación Ramón Areces and of the Generalitat Valenciana, respectively.

References

Altona, C. & Sundaralingam, M. (1972). *J. Am. Chem. Soc.* **94**, 8205–8212.
Arnott, S. & Hukins, D. W. L. (1969). *Nature (London)*, **224**, 886–888.
Cunin, R., Glansdorff, N., Piérard, A. & Stalon, V. (1986). *Microbiol. Rev.* **50**, 314–352.
Esnouf, R. M. (1999). *Acta Cryst.* D**55**, 938–940.
Ghosh, M., Meerts, I. A., Cook, A., Bergman, A., Brouwer, A. & Johnson L. N. (2000). *Acta Cryst.* D**56**, 1085–1095.
Gil, F., Ramón-Maiques, S., Marina, A., Fita, I. & Rubio, V. (1999). *Acta Cryst.* D**55**, 1350–1352.
Jones, T. A., Zou, J., Cowan, S. & Kjeldgaard, M. (1991). *Acta Cryst.* A**47**, 110–119.
Kraulis, P. J. (1991). *J. Appl. Cryst.* **24**, 946–950.
Merritt, E. A. & Murphy, M. E. P. (1994). *Acta Cryst.* D**50**, 869–873.
Murshudov, G. N., Vagin, A. A. & Dodson, E. J. (1997). *Acta Cryst.* D**53**, 240–255.
O'Sullivan, W. J. & Smithers, G. W. (1979). *Methods Enzymol.* **63**, 294–336.
Phillippsen, A. (1998). *DINO: a Realtime Visualization Program for Structural Biology Data*. http://www.bioz.unibas.ch/~xray/dino.
Ramón-Maiques, S., Marina, A., Gil-Ortiz, F., Fita, I. & Rubio, V. (2002). *Structure*, **10**, 329–342.
Saenger, W. (1984). *Principles of Nucleic Acid Structure.* New York: Springer–Verlag.
Vetter, I. R. & Wittinghofer, A. (1999). *Q. Rev. Biophysics*, **32**, 1–56.
Wallace, A. C., Laskowski, R. A. & Thorton, J. M. (1995). *Protein Eng.* **8**, 127–134.
Yount, R. G., Babcock, D., Ballantyne, W. & Ojala, D. (1971). *Biochemistry*, **10**, 2484–2489.